Journal of the European Ceramic Society 17 (1997) 13–24

PII: S0955-2219(96)00075-1
0955-2219/97/$17.00

Grain Morphology and Intergranular Microstructure of Whisker Reinforced Si_3N_4 Ceramics

Håkan Björklund & Lena K. L. Falk

Department of Physics, Chalmers University of Technology, S-412 96 Göteborg, Sweden

(Received 8 January 1996; revised version received 25 March 1996; accepted 2 April 1996)

Abstract

The effect of metal oxide and whisker additions on the grain morphology and intergranular microstructure of Si_3N_4-based ceramic materials has been characterized by analytical electron microscopy in combination with quantitative microscopy. The Si_3N_4 ceramics were formed either without metal oxide sintering additives or with 2·5 wt% Y_2O_3 and 0·2 wt% Fe_2O_3. SiC or β-Si_3N_4 whiskers were added to these two compositions.

The microstructural analysis showed that both metal oxide and whisker additions affect the Si_3N_4 microstructure. The addition of Y_2O_3 and Fe_2O_3 promoted the development of a fibrous β-Si_3N_4 matrix with a larger fraction of intergranular amorphous phase. The presence of SiC whiskers suppressed β-Si_3N_4 grain growth during densification while an addition of β-Si_3N_4 whiskers resulted in a coarser microstructure.

The different microstructures were related to the mechanical properties of the ceramics and the results imply that the matrix microstructure has a significant influence upon the mechanical behaviour of Si_3N_4-based ceramic composites. © 1996 Elsevier Science Limited.

1 Introduction

It was recognized early that grain morphology has a crucial influence upon the mechanical properties of Si_3N_4 ceramics. Work by Lange demonstrated that development of a fibrous microstructure containing prismatic β-Si_3N_4 grains promotes formation of an Si_3N_4 ceramic material with high room-temperature strength and toughness.[1] More recent work has demonstrated that it is possible to tailor Si_3N_4 microstructures through choice of metal oxide sintering additives.[2–4] At elevated temperatures the metal oxide additives react with the SiO_2 present on the Si_3N_4 starting powder particles and some of the Si_3N_4 to form an oxynitride liquid phase, which serves as mass transport medium during densification.[1,5,6] The α-Si_3N_4 in the starting powder is preferentially dissolved in this liquid and reprecipitates as β-Si_3N_4. The chemistry, and volume, of the oxynitride liquid phase sintering medium will determine the grain morphology and intergranular microstructure of the sintered material.[3–5] It has been shown that certain oxide additives form an oxynitride liquid phase that promotes growth of prismatic β-Si_3N_4 grains with hexagonal cross-section. Development of these microstructures enabled the fabrication of 'self-reinforced' Si_3N_4 ceramics with improved strength and toughness both at low and high temperatures.[4] However, the mechanical and chemical properties of the ceramic will, in addition to Si_3N_4 grain morphology, also be governed by the distribution and composition of secondary crystalline and amorphous phases. A certain amount of the liquid phase sintering medium is generally retained as thin amorphous grain boundary films also in systems where secondary crystalline phases partition from the liquid during densification.[1,5,7]

The inherent brittle behaviour and flaw sensitivity of most ceramic materials may be controlled by the addition of a reinforcing agent. SiC and β-Si_3N_4 whiskers have been incorporated into Si_3N_4 ceramic microstructures in order to improve toughness and fracture resistance.[8–12] Among the mechanisms proposed for the observed toughening effect are crack deflection by the whiskers and whisker debonding, bridging and pull-out.[13] The operation of these energy-dissipative mechanisms will be dependent upon the chemistry of the interface, i.e. the bond strength; debonding of the reinforcing phase is a necessary requirement for crack deflection, bridging and pull-out.[9] These toughening mechanisms are likely to be responsible also for the improved properties of the 'self-reinforced' Si_3N_4 materials. The mechanical behaviour of a whisker reinforced Si_3N_4 ceramic will, however,

also be dependent upon the matrix morphology. Matrix grain size and shape, in relation to the size and shape distributions of the reinforcement, as well as the intergranular microstructure will also have an influence on the properties of these composite materials.[8,14]

The present paper is concerned with the effect of metal oxide and whisker additions on β-Si_3N_4 grain morphology and intergranular microstructure of Si_3N_4 ceramics. The materials were densified by hot-isostatic pressing (HIP), which makes it possible to form a dense and isotropic material with only small amounts of metal oxide sintering additives.[2,10] The β-Si_3N_4 grain size and shape distributions were studied with the aid of quantitative microscopy in combination with a stereological method.[15] The detailed microstructure, particularly the intergranular structure, was investigated by analytical electron microscopy.

2 Experimental Procedures

2.1 Materials

The experimental Si_3N_4 materials in this investigation are shown in Table 1. The Si_3N_4 starting powder was UBE SN 10, which contains 97% α-Si_3N_4 and has an oxygen content that corresponds to 2·4 wt% surface SiO_2. The Si_3N_4 ceramics were densified without metal oxide additives or with an addition of 2·5 wt% Y_2O_3 and 0·2 wt% Fe_2O_3. SiC whiskers (Tateho, SCW#1) or β-Si_3N_4 whiskers (UBE-SN-WB) were incorporated into these two matrices. Unreinforced ceramics were also studied as reference materials. Densification was carried out by HIP using the glass encapsulation technique. The addition of metal oxides made it possible to obtain fully dense materials at a lower temperature and with a reduced pressure during a shorter period of time, see Table 1. Detailed descriptions of the preHIP processing and mechanical testing of these Si_3N_4 ceramics are given elsewhere.[10] Preliminary investigations of the microstructures have been reported previously.[16–18]

The microstructural characterization was carried out by analytical scanning and transmission electron microscopy (SEM/TEM/STEM/EDX)* in combination with quantitative microscopy. Phase compositions were determined by X-ray diffractometry of polished sections. The relative amount of Si_2N_2O in the materials was estimated by the peak height ratio (S):

$$S = Si_2N_2O[(110) + (200)] / \{Si_2N_2O[(110) + (200)] + \beta\text{-}Si_3N_4\,[(100) + (110)]\} \quad (1)$$

*CamScan 4S-80DV SEM, Link eXL; Jeol 2000-FX TEM/STEM/SEM, Link AN 10 000.

2.2 Scanning electron microscopy

Polished and etched sections were examined in the scanning electron microscope (SEM). Etching was carried out in molten NaOH at 450°C for 10–30 s. This technique removes, preferentially, the intergranular glassy phase, and makes it possible to distinguish separate grain sections. The ceramics containing SiC whiskers were plasma-etched using CF_4 gas prior to etching in NaOH. This made it possible to distinguish the SiC whiskers from the Si_3N_4 grains in the SEM. Plasma etching attacks primarily the Si_3N_4 and Si_2N_2O, leaving the SiC and the integranular regions as elevated areas. The etched sections were coated with a thin evaporated carbon film to avoid charging under the electron beam and imaged in the SEM by backscattered electrons.

2.3 Quantitative microscopy

The β-Si_3N_4 grain size and shape distributions of the materials were estimated by quantitative microscopy. Enlarged SEM micrographs (final magnification 12000–40000×) of the etched sections were placed on a digitizing tablet (HP 9874A) linked to a computer and the positions of the individual grain section corners were registered.[15] The Si_3N_4 grain corners were defined by manually marking grain boundaries and identifying SiC whiskers prior to measurement. Four hundred to five hundred grain sections were measured for each material.

These measurements were used for determination of the following two-dimensional parameters describing the individual β-Si_3N_4 grain sections: grain section maximum dimension (D_m) which is the longest distance between two corners of a grain section, number of corners (N_c) and a dimensionless shape parameter ($Q = 4\pi$ area /(perimeter)^2).

The distribution of measured D_m values and the mean values of maximum dimension ($\overline{D}_m$), corners per grain section ($\overline{N}_c$) and the shape parameter ($\overline{Q}$) were then determined for the different materials. The spread in the distribution of measured maximum dimensions was determined by $s/\overline{D}_m$, where s is the standard deviation in the determination of $\overline{D}_m$. The precision in $\overline{D}_m$ was determined with a 95% confidence interval.

The grain shape distributions of the materials were assessed through comparison of the experimental stereological parameters with computer-generated stereological parameters. The method is based on the assumption that the shape of the β-Si_3N_4 grains in these materials can be approximated by hexagonal prisms and that the aspect ratio distribution within a β-Si_3N_4 microstructure can be represented by its mean value.[15] The aspect ratio of a grain is the ratio between its length and width. The width was, in the present investigation,

Table 1. Powder composition, process conditions and phase composition of the examined materials

Oxide addition	*Whisker addition (wt%)*	*Densification process*			*Phase composition*	S-*value*
		T*(°C)*	t *(h)*	P *(MPa)*		
UD	–	1950	2	250	β-Si_3N_4	0
UD	25 SiC	1950	2	250	β-Si_3N_4, Si_2N_2O, β-SiC	0·2
UD	25 β-Si_3N_4	1950	2	250	β-Si_3N_4, Si_2N_2O	0·2
LD	–	1775	1	200	β-Si_3N_4, Si_2N_2O	0·1
LD	25 SiC	1775	1	200	β-Si_3N_4, Si_2N_2O, β-SiC	0·1
LD	25 β-Si_3N_4	1775	1	200	β-Si_3N_4, Si_2N_2O, β-$Y_2Si_2O_7$	0·1
LD	35 β-Si_3N_4	1775	1	200	β-Si_3N_4, Si_2N_2O, α-$Y_2Si_2O_7$	0·1

UD: No addition of metal oxides.
LD: Addition of 2·5 wt% Y_2O_3 and 0·2 wt% Fe_2O_3.
S = relative amount of Si_2N_2O in the material, estimated as per eqn (1).

defined as the distance between two opposite corners on the hexagonal cross-section perpendicular to the length. This stereological method has previously been described in detail for different grain shapes.[15,19]

2.4 Transmission electron microscopy

Thin foils for transmission electron microscopy (TEM) were prepared by standard techniques, and coated with a thin evaporated carbon film to avoid charging under the electron beam. The presence of grain boundary films was determined by Fresnel out-of-focus imaging and dark-field imaging using diffuse scattered electrons.[20] The latter technique reveals the distribution of amorphous phases in the microstructure.

3 Results

3.1 β-Si_3N_4 grain morphology

X-ray diffraction (XRD) patterns from the materials in Table 1 did not show any reflections from retained α-Si_3N_4. This shows that the α- to β-Si_3N_4 phase transformation during densification was virtually complete in the materials formed with and without the metal oxide sintering additives. The mean values of maximum dimension ($\overline{D}_m$) corners per grain section ($\overline{N}_c$) and the shape parameter ($\overline{Q}$), and the spread in the distribution of measured maximum dimensions ($s/\overline{D}_m$) determined for the experimental materials, are given in Table 2.

3.1.1 Grain morphology of reference materials

The material formed without metal oxides showed mainly equiaxed grain sections in the SEM. Only a few sections had an elongated shape, Fig. 1(a). The material fabricated with the addition of metal oxides had a larger number of smaller grain sections and a more fibrous microstructure, Fig. 1(b). Steric hindrance of growing β-Si_3N_4 grains was observed in both types of matrix.

The material formed with the metal oxide additives had a significantly lower $\overline{D}_m$ value than the material formed without the metal oxides, 0·39 μm compared with 0·51 μm, Table 2 and Figs. 2(a) and (c). In the material formed with the metal oxides, 63% of the observed grain sections had maximum dimensions smaller than 0·375 μm, while only 37% of the grain sections in the material formed without the metal oxides were in that range. The maximum dimension distribution of the material formed with the metal oxides exhibited a certain amount of larger sections despite the lower mean maximum dimension, Fig. 2(c). This was also reflected in a higher value of $s/\overline{D}_m$ for this material, Table 2.

Table 2. Mean grain section maximum dimensions ($\overline{D}_m$), spread in D_m distributions ($s/\overline{D}_m$) and mean value of shape parameters ($\overline{Q}$) and number of corners/grain section ($\overline{N}_c$) for the examined material

Powder composition	$\overline{D}_m$ (μm)	$s/\overline{D}_m$	$\overline{Q}$	$\overline{N}_c$
UD	0·51 ± 0·03	0·58	0·722	5·38
UD + 25 SiC	0·43 ± 0·02	0·42	0·728	4·85
UD + 25 β-Si_3N_4	0·97 ± 0·07	0·69	0·727	5·75
LD	0·39 ± 0·03	0·77	0·727	5·34
LD + 25 SiC	0·38 ± 0·02	0·50	0·718	5·17
LD + 25 β-Si_3N_4	0·86 ± 0·08	1·05	0·707	5·26
LD + 35 β-Si_3N_4	0·66 ± 0·06	0·92	0·728	6·25

UD: No addition of metal oxides.
LD: Addition of 2·5 wt% Y_2O_3 and 0·2 wt% Fe_2O_3.

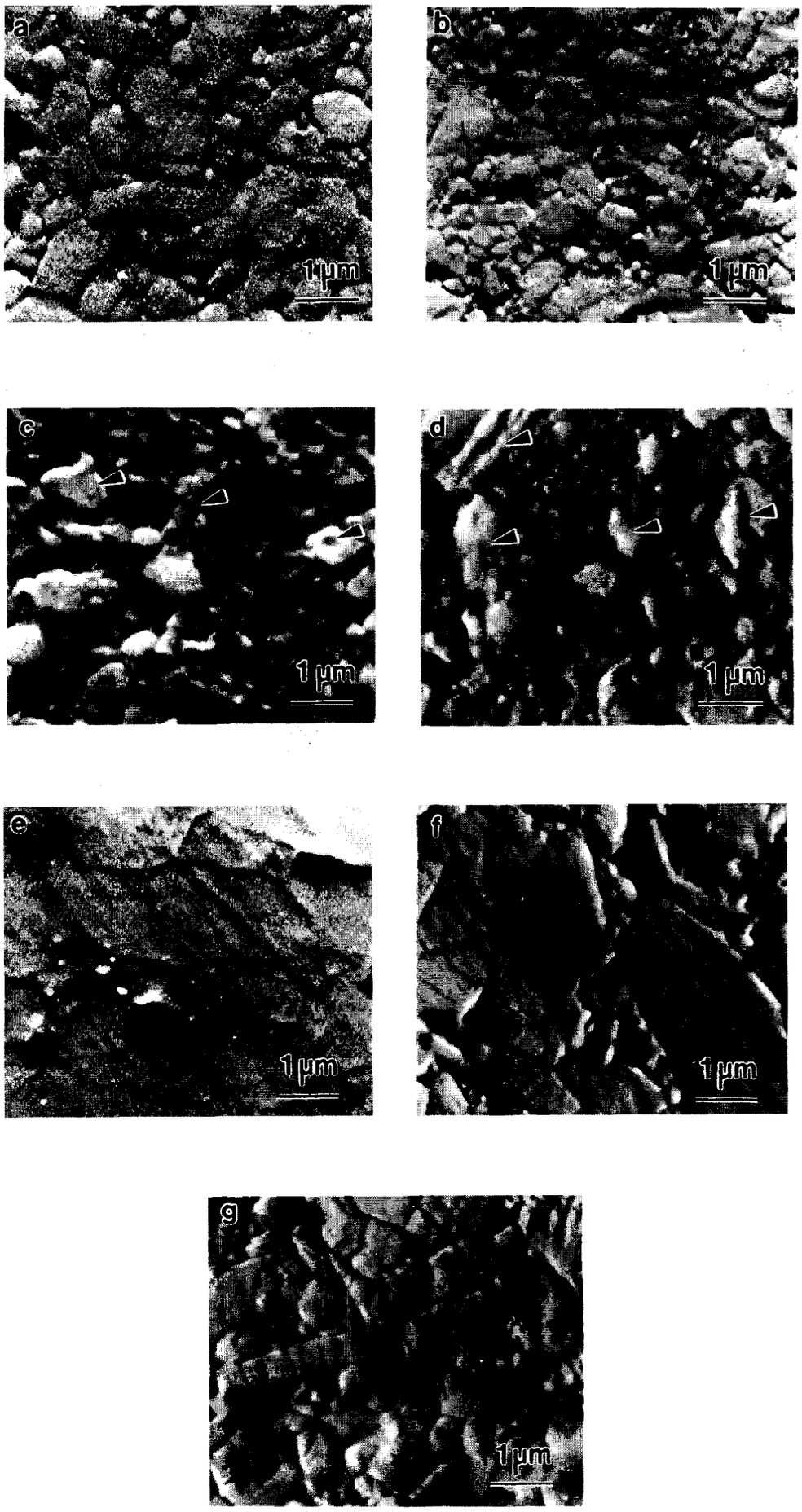

Fig. 1. SEM images formed by backscattered electrons showing sections of the Si_3N_4 reference materials formed without (a) and with (b) the metal oxides, (c) Si_3N_4 formed with 25 wt% SiC whiskers (arrowed), (d) Si_3N_4 formed with the metal oxides and 25 wt% SiC whiskers (arrowed), (e) Si_3N_4 formed with 25 wt% β-Si_3N_4 whiskers, and Si_3N_4 formed with the metal oxides and 25 (f) or 35 (g) wt% β-Si_3N_4 whiskers.

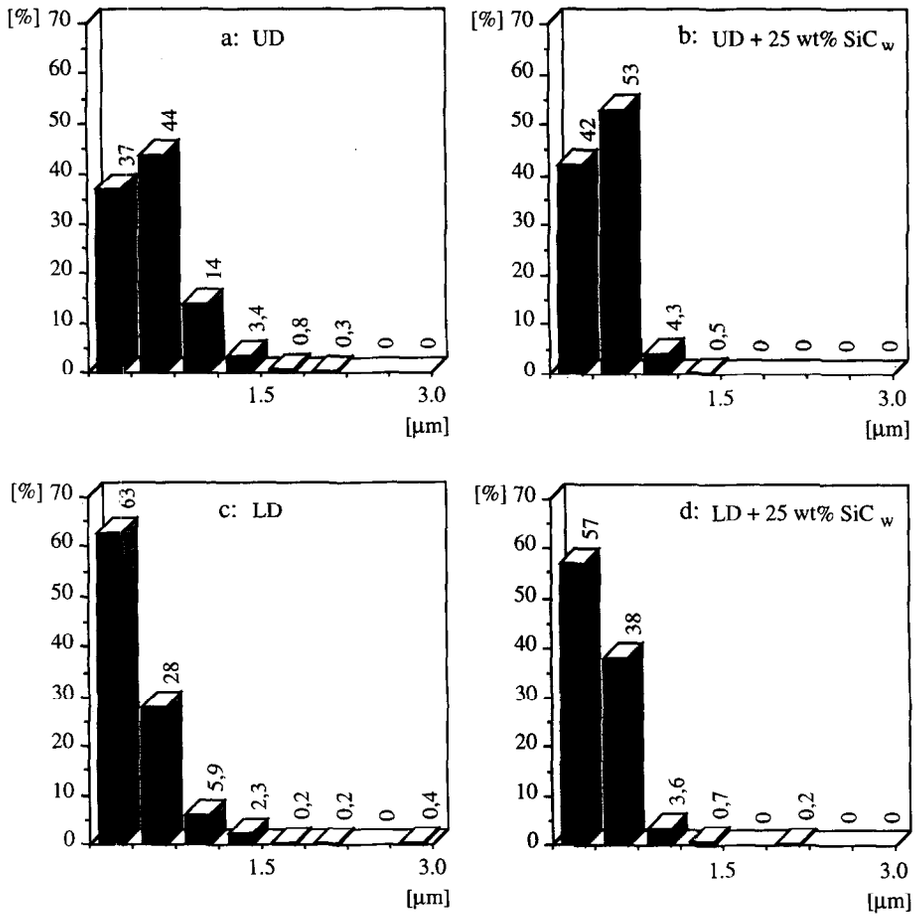

Fig. 2. Matrix grain section maximum dimension (D_m) distributions for the reference materials (a, c) and for the SiC whisker reinforced materials (b, d). One bar represents an interval of 0.375 μm and the heights of the bars show observed frequency.

3.1.2 Grain morphology of SiC whisker containing materials

SEM indicated that there was also a clear difference between the two β-Si_3N_4 matrix grain morphologies when 25 wt% SiC whiskers was added, Figs 1(c) and (d). The composite formed with the metal oxides did also have a slightly lower $\overline{D}_m$ value, see Table 2. The addition of SiC whiskers resulted in a reduced spread in the distributions of measured maximum dimension (D_m) for the two matrices, see Table 2. This is also evident when comparing the diagrams in Figs 2(a) and (c) with Figs 2(b) and (d), respectively; it can be noted that only 5% of the measured D_m values were larger than 0·75 μm in the two matrices when the SiC whiskers had been added. There was also a pronounced reduction in $\overline{D}_m$ when the SiC whiskers were added to the matrix formed without the metal oxides, from 0·51 to 0·43 μm, see Table 2.

3.1.3 Grain morphology of β-Si_3N_4 whisker containing materials

The materials formed with β-Si_3N_4 whiskers had much coarser microstructures than the other materials, Figs 1(a), (b) and (c). SEM showed that the materials formed with additions of β-Si_3N_4 whiskers together with the metal oxides contained larger grains separated by fine-grained areas, Figs 1(b) and (c).

These coarse microstructures had significantly higher mean maximum dimensions and a larger spread in the maximum dimension distributions than the other materials, see Table 2 and Fig. 3. The addition of 25 wt% β-Si_3N_4 whiskers resulted in $\overline{D}_m$ = 0·97 μm and an $s/\overline{D}_m$ value of 0·69 without the metal oxide additives. The mean maximum dimension ($\overline{D}_m$) decreased from 0·86 to 0·66 μm when the β-Si_3N_4 whisker addition to the metal oxide containing matrix increased from 25 to 35 wt%. This decrease in $\overline{D}_m$ was accompanied by a reduction in the $s/\overline{D}_m$ value, from 1·05 to 0·92.

3.2 Intergranular microstructure

The three materials formed without the metal oxide additives contained thin amorphous films separating adjacent β-Si_3N_4 grains and SiC whiskers from the Si_3N_4 matrix, Figs 4(a) and 5. Only smaller glass pockets, rich in Si and O, could be observed at multigrain junctions in these materials. The addition of the metal oxides resulted in an increased amount of residual intergranular glass. Amorphous intergranular films merged into larger Y–, Si- and O-rich glass pockets at multigrain junctions, Fig. 4(b). The Fe originating from

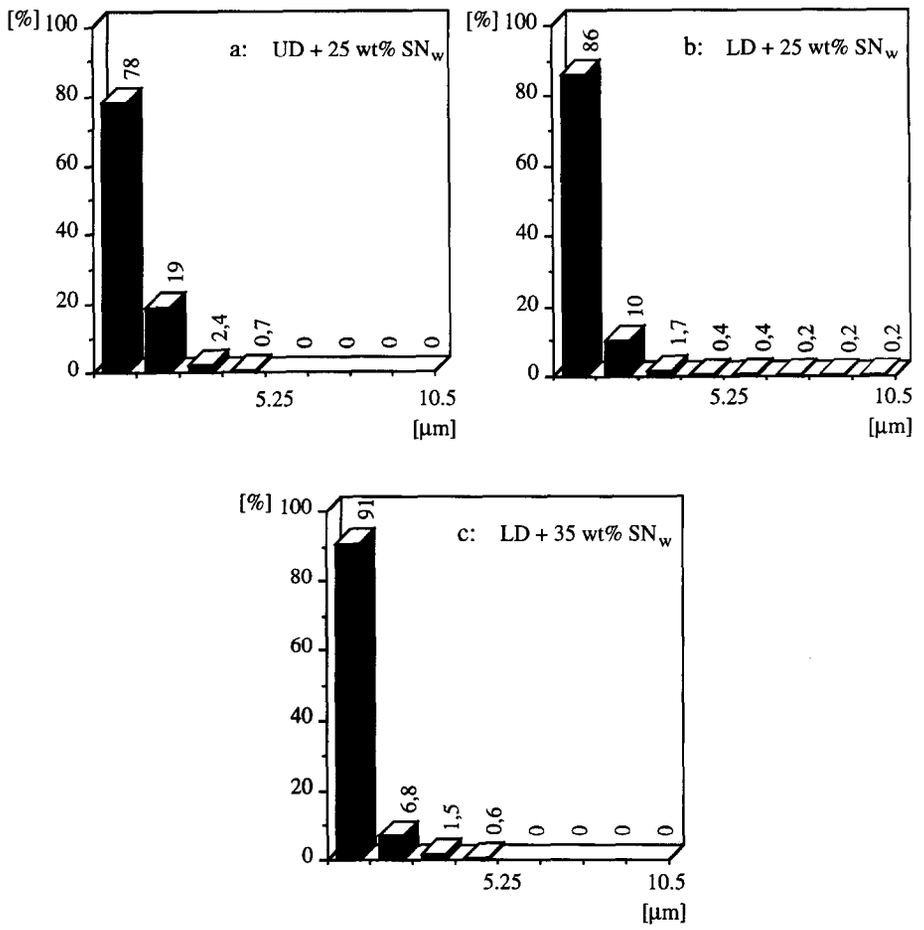

Fig. 3. Grain section maximum dimension (D_m) distributions in the materials formed with β-Si_3N_4 whiskers without (a) and with the metal oxides (b, c). One bar represents an interval of 1·313 μm.

the Fe_2O_3 was concentrated to smaller Fe-rich intergranular particles. Energy-dispersive X-ray (EDX) analysis and selected area electron diffraction in the TEM indicated that these particles were Fe silicides.

XRD showed that additions of metal oxides and whiskers resulted in the formation of smaller amounts of Si_2N_2O, see Table 1. The materials formed with the metal oxides had a lower relative Si_2N_2O content than the whisker reinforced materials formed without the metal oxides. Only a few Si_2N_2O grains were identified by TEM in the Si_2N_2O-containing materials. The observed Si_2N_2O grains had the typical faulted structure and their identity was determined by EDX and electron diffraction, Fig. 6.

The intergranular microstructure was also affected by the addition of β-Si_3N_4 whiskers. The addition of 25 wt% β-Si_3N_4 whiskers to the material formed without the metal oxide additives resulted in a local formation of Y–S–O-rich glass pockets. $Y_2Si_2O_7$ formed in addition to the Y–Si–O-rich residual glass phase when the β-Si_3N_4

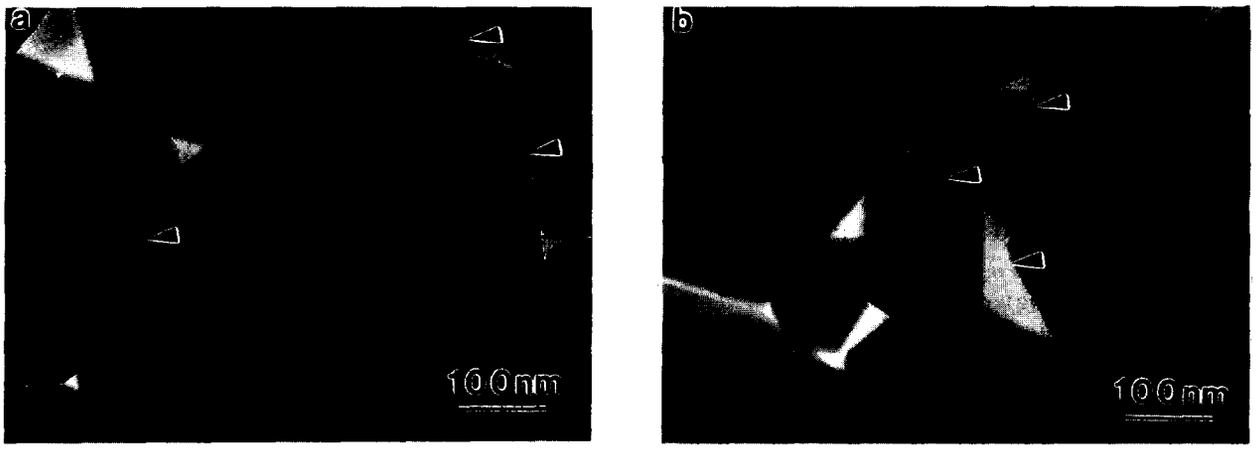

Fig. 4. TEM centred dark-field images formed using diffuse scattered electrons. The intergranular glassy phase appears bright (arrowed). The reference materials formed (a) without additives and (b) with the metal oxides.

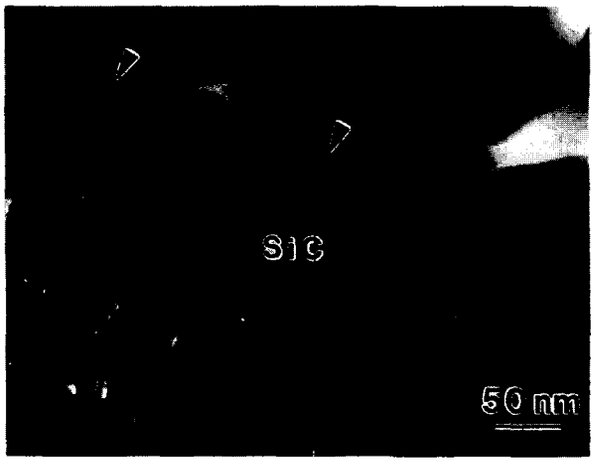

Fig. 5. TEM centred dark-field image formed using diffuse scattered electrons of a boundary between an SiC whisker and the matrix in the SiC whisker reinforced material formed without the metal oxides. A thin amorphous film (arrowed) is separating the whisker from the matrix.

whiskers were added together with the metal oxides. XRD indicated that the $Y_2Si_2O_7$ was of the β polymorph in the material with 25 wt% β-Si_3N_4 whiskers but of the α polymorph when 35 wt% whiskers were added.

The SiC whiskers contained, in some cases, cavities associated with a surface layer of a Ca-rich amorphous phase, Fig. 7(a). These cavities had, in general, grown to larger volumes containing an Si-, Y-, Ca- and O-rich glassy phase when the SiC whiskers had been added together with the metal oxides, Fig. 7(b).

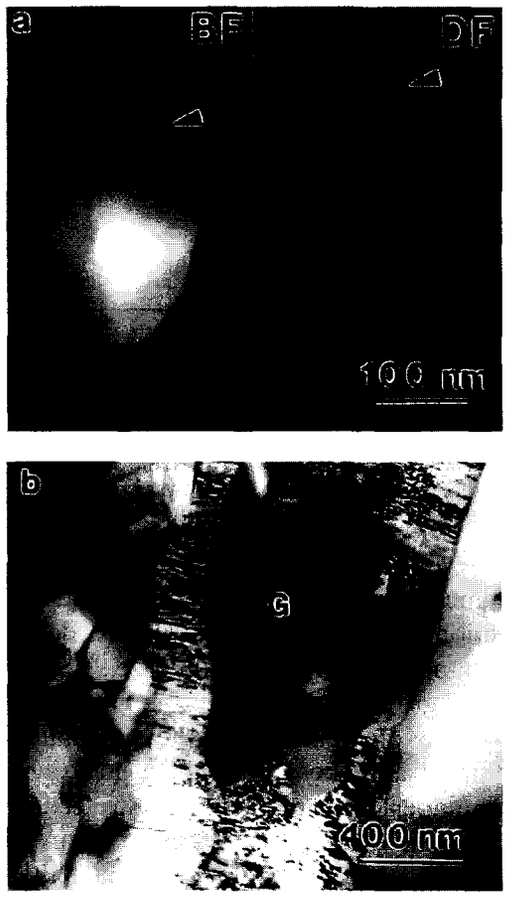

Fig. 7.. (a) Bright-field (BF) and centred dark-field (DF) TEM images of whisker cavity associated with a Ca-rich amorphous phase (arrowed) in the material formed without metal oxides. The DF image was formed using diffuse scattered electrons and the amorphous phase appears bright. (b) TEM image of SiC whisker in the material formed with the metal oxides, showing the presence of larger glassy zones associated with the whisker (G).

4 Discussion

4.1 Interpretation of measured two-dimensional parameters

The quantitative measurements were carried out in order to determine the effect of whisker additions upon the two different β-Si_3N_4 matrix microstructures. The two-dimensional parameter D_m was chosen for this characterization because the D_m distribution is heavily biased towards its maximum value and the distribution converges relatively quickly. It has been shown that the measurement of 400 grain sections is sufficient to establish the D_m distribution in these types of microstructure.[15,19]

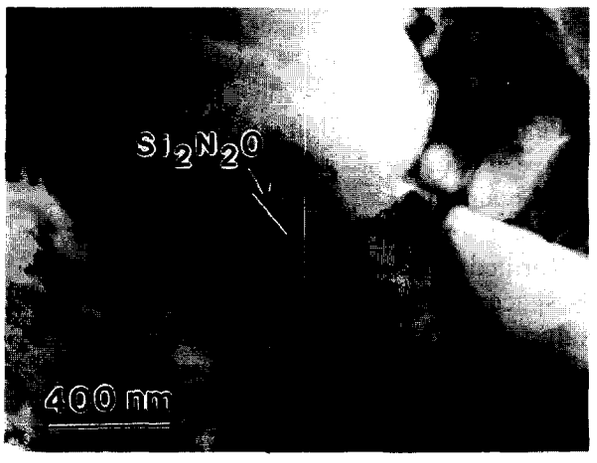

Fig. 6. TEM image of an Si_2N_2O grain in the material formed with 35 wt% β-Si_3N_4 whiskers and the metal oxides.

The grain section maximum dimension distribution and $\overline{D}_m$ will be determined by β-Si_3N_4 grain shape as well as grain size. $\overline{D}_m$ calculated for a large number of computer-generated random sections through a hexagonal prism is shown as function of aspect ratio in Fig. 8, where the prism volume is kept constant. These results would describe modelled microstructures consisting of monosized prisms, but it can be assumed that the variation in $\overline{D}_m$ with mean aspect ratio in a true microstructure is similar.[15] This indicates that the aspect ratio of the β-Si_3N_4 grains must be considered when evaluating variations in mean maximum dimension ($\overline{D}_m$) and D_m distribution in relation to grain volume.

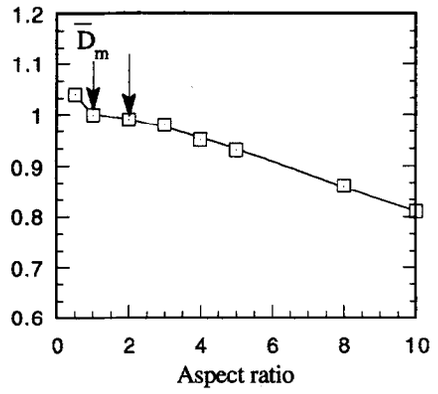

Fig. 8. Calculation of expected mean grain section maximum dimension as function of aspect ratio for hexagonal prisms of unit volume. The range of $\bar{D}_m$ values determined for the experimental materials is indicated by arrows. Data from Ref. 15

The mean values $\bar{N}_c$ and $\bar{Q}$ on a random vertical section through a microstructure depend on grain shape but not on grain size.[19] Steric hindrance of growing β-Si_3N_4 grains may result in a grain shape diverging from the postulated prismatic shape and thereby result in an exaggerated mean number of corners per grain section. The experimentally determined values of mean number of corners per grain section ($\bar{N}_c$) may, therefore, deviate significantly from those generated for modelled microstructures consisting of monosized prismatic grains with a given aspect ratio. However, the experimental $\bar{Q}$ values would only show minor deviations from the values obtained by theoretical modelling.[15,19] A comparison of the experimental $\bar{Q}$ data with computer-generated plots of $\bar{Q}$ as function of aspect ratio for modelled microstructures consisting of monosized grains would thus enable the prediction of a mean aspect ratio of the β-Si_3N_4 grains in the experimental materials.[15,19] The $\bar{Q}$ versus aspect ratio plot in Fig. 9 was obtained by computer simulations involving the generation of a large number of random sections through hexagonal prisms with different aspect ratios.[15]

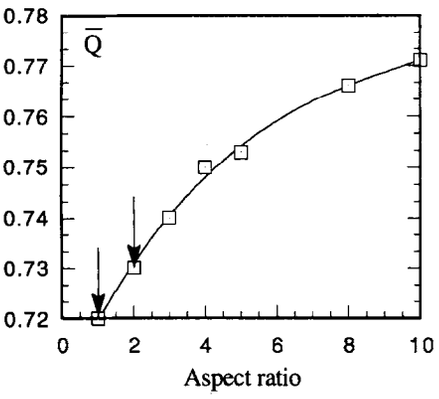

Fig. 9. Expected mean value of shape parameter, $\bar{Q}$, for hexagonal prisms as a function of their aspect ratio. The range of $\bar{Q}$ values determined for the experimental materials is indicated by arrows. Data from Ref. 15

It, can be noted that small differences in experimental $\bar{Q}$ will have a significant effect on the proposed mean aspect ratio of the grains, see Fig. 9. It is therefore difficult to assess the significance of the different $\bar{Q}$ values for these experimental materials in terms of a varying mean aspect ratio. A comparison of the experimental $\bar{Q}$ values in Table 2 with the computer-generated plot in Fig. 9 implies, however, that the mean aspect ratios of the experimental materials in the present investigation are in the range 1 to 2. (The lower $\bar{Q}$ value, 0·707, of the material fabricated with 25 wt% β-Si_3N_4 whiskers in addition to the metal oxides does probably reflect the presence of larger and extremely irregular grain sections in this material.)

A variation of aspect ratio in the suggested range will only have a small effect upon the $\bar{D}_m$ value as shown by the computer-generated plot in Fig. 8. It is therefore concluded that the difference in $\bar{D}_m$ between the two reference materials and the change in $\bar{D}_m$ when whiskers were added (Table 2) to these matrices are due, primarily, to different β-Si_3N_4 grain volume distributions.

4.2 Development of β-Si_3N_4 grain morphology

4.2.1 Reference materials

The results imply that the reference Si_3N_4 material fabricated with the metal oxide additives had a smaller mean grain size and a broader grain size distribution than the material formed without additives, see Table 2 and Fig. 2. The larger mean grain size in the material formed without the metal oxides could be expected due to the prolonged time at a higher temperature during densification. Of the observed grain sections in the reference material formed with the metal oxides, 63% had D_m values smaller than 0·375 μm which indicates that this material contained a larger number of smaller grains. However, this material also contained a fraction of larger β-Si_3N_4 grains as indicated by the tail in the D_m distribution, Fig. 2(c). This type of microstructure could possibly be caused by an increased nucleation in a larger liquid volume and the different composition of the oxynitride liquid phase present during densification. Previous investigations indicate that the addition of Y_2O_3 as a sintering additive is sometimes associated with microstructures containing larger elongated β-Si_3N_4 grains.[2,4,21,22] The lower amount of liquid present in the material formed without metal oxides would restrict the space available for grain growth, thereby resulting in a narrower grain size distribution.

The results from the characterization of the Si_3N_4 materials in this investigation imply that the additions of SiC and β-Si_3N_4 whiskers have a pronounced effect on the development of these Si_3N_4 matrix microstructures.

4.2.2 SiC whisker reinforced materials

The addition of SiC whiskers resulted in a reduction of the tails of the D_m distributions for both types of matrix; 95% of the measured grains had a D_m less than 0.75 μm in each material, Fig. 2. It may therefore be concluded that the SiC whisker addition suppressed Si_3N_4 matrix grain growth. The results also suggest that the extent to which grain growth is suppressed is dependent upon the overall Si_3N_4 matrix composition, and possibly also densification temperature. No significant change in $\bar{D}_m$ was observed for the Si_3N_4 matrix when the metal oxides had been added, and the change in the D_m distribution was less dramatic, see Table 2 and Figs 2(c) and (d). However, there was a significant reduction in $\bar{D}_m$ when SiC whiskers were added to the Si_3N_4 matrix without the addition of the metal oxides. This would be consistent with a reduced Si_3N_4 mean grain size due to the presence of the SiC whiskers.

These observations lend support to earlier reports that SiC whiskers and particles hinder Si_3N_4 grain growth.[11,12,23] Probable mechanisms could be a different composition of the liquid phase due to exsolution of impurities or carbon from the whiskers or steric hindrance of growing β-Si_3N_4 grains by the SiC whiskers.[11] Also, the addition of SiC whiskers would change the amount of liquid phase, i.e. the volume fraction of the transport medium, present during densification. It has been reported that grain growth during liquid phase sintering can be obstructed by a second phase.[24]

4.2.3 Si_3N_4 whisker reinforced materials

The significantly higher $\bar{D}_m$ values determined for the three materials formed with β-Si_3N_4 whiskers imply a pronounced increase in β-Si_3N_4 grain size, see Table 2 and Fig. 3. These microstructures indicate that exaggerated grain growth, promoted by the whisker addition, took place during densification.

The microstructure of the material formed with 25 wt% β-Si_3N_4 whiskers but without the metal oxides appeared to be comparatively homogeneous but coarser than that of the other materials, see Figs 1(e), 2(a) and 3. The larger grain sizes in this material may be expected owing to the prolonged time at a higher temperature during densification. The β-Si_3N_4 whisker reinforced materials formed with the metal oxides contained larger β-Si_3N_4 grains dispersed in a fine-grained matrix, as shown in Fig. 1(f) This suggests that the β-Si_3N_4 whiskers grew extensively during densification, resulting in an apparent bimodal grain size distribution where the larger β-Si_3N_4 grains originated from the whisker addition. Similar microstructures of β-Si_3N_4 whisker reinforced Si_3N_4 have been reported earlier.[25,26]

$\bar{D}_m$ was reduced when the β-Si_3N_4 whisker addition was increased from 25 to 35 wt%, but the value was still significantly higher than that determined for the unreinforced material. A reduced volume fraction of oxynitride liquid due to a larger whisker volume would make transport of dissolved Si_3N_4 more difficult and thereby decrease grain growth rate. The development of very large grains may also be suppressed by the increased fraction of β-Si_3N_4 whiskers which would restrict the space available for grain growth and thus increase the effect of steric hindrance, thereby reducing the grain size.

4.3 Intergranular microstructure

The formation of an oxynitride liquid phase sintering medium in the materials formed without the metal oxides was promoted by the surface silica present on the starting powder particles. The low volume fraction of a residual intergranular glassy phase in these materials suggests that the volume fraction of liquid present during sintering was comparatively small despite the high densification temperature. However, it may be expected that the volume fraction of the liquid phase present during densification is larger than the volume fraction of the residual intergranular glassy phase.[1] A complete transformation of α- to β-Si_3N_4 was achieved during densification, but, still, the space available for grain growth in the liquid phase environment would be restricted and result in steric hindrance of the growing β-Si_3N_4 grains.

TEM showed that the oxynitride liquid phase may react with the SiC whiskers during the densification process and this was more pronounced when the metal oxides had been added. It has been proposed previously that liquid SiO_2 and also metal oxides such as Y_2O_3 can react with solid SiC.[27] A characterization of this type of SiC whiskers showed that they contain impurities such as Al, Ca and Fe,[28] and it is likely that these impurities promote the reaction between the SiC whiskers and the liquid phase.[29]

The presence of a Y–Si–O–rich residual glass and $Y_2Si_2O_7$ in the β-Si_3N_4 whisker reinforced materials was caused by impurity Y originating from the whiskers.[30] It is possible that a larger amount of Y will stabilize the α-polytype, which may explain why α-$Y_2Si_2O_7$ was formed when 35 wt% β-Si_3N_4 whiskers were added together with the metal oxides. Moreover, the Fe-rich particles present in the β-Si_3N_4 whisker reinforced material fabricated without the addition of metal oxides was caused by impurity Fe also originating from the whiskers.[30]

An increased oxygen content caused by the metal oxides and impurities in the whisker materials resulted in the formation of Si_2N_2O.[28,30] XRD indicated that the volume fractions of Si_2N_2O were very small, and it was therefore assumed that any influence of Si_2N_2O on the grain section measurements could be disregarded. In a previous characterization of β-Si_3N_4 materials, the Si_2N_2O was observed to develop grains substantially larger than the surrounding Si_3N_4 grains.[7] However, TEM as well as SEM did not indicate that the Si_2N_2O grains formed in these materials had this morphology, Fig. 6.

4.4 Relation between microstructure and mechanical properties

The results from measurements of strength and indentation fracture toughness imply that the Si_3N_4 matrix grain morphology and intergranular microstructure have a clear effect on the mechanical properties,[10] Fig. 10.

Crack propagation has previously been studied in these materials.[32] Room-temperature fracture surfaces studied by SEM and cracks originating from Vickers indentation marks studied by SEM and TEM indicated that the fracture is mainly intergranular. Crack deflection, crack bridging and pull-out by Si_3N_4 grains or whiskers are possible toughening mechanisms.[32] The contribution from the different toughening mechanisms will depend upon the size and shape distributions of the β-Si_3N_4 grains as well as the presence of whiskers.

The whisker additions to the β-Si_3N_4 matrix formed without the metal oxide sintering additives had a clear toughening and strengthening effect at room temperature as shown in Fig. 10. However, the addition of SiC whiskers together with the metal oxides did not result in any significant change in toughness and strength. This could possibly be explained by the altered Si_3N_4 matrix microstructure; the SiC whiskers effectively suppressed the fraction of larger β-Si_3N_4 grains. It may be assumed that larger, and elongated, β-grains will contribute more to fracture toughness than smaller grains.[12,33] This would result in a higher fracture toughness of the monolithic material than of the Si_3N_4 matrix in the SiC whisker reinforced material, which may explain why the addition of 25 wt% SiC whiskers did not increase fracture toughness in this case.

The reduced strength of the materials fabricated with β-Si_3N_4 whiskers and the metal oxides implies that the larger β-Si_3N_4 grains, which give a certain toughening effect, may act as flaws.[33]

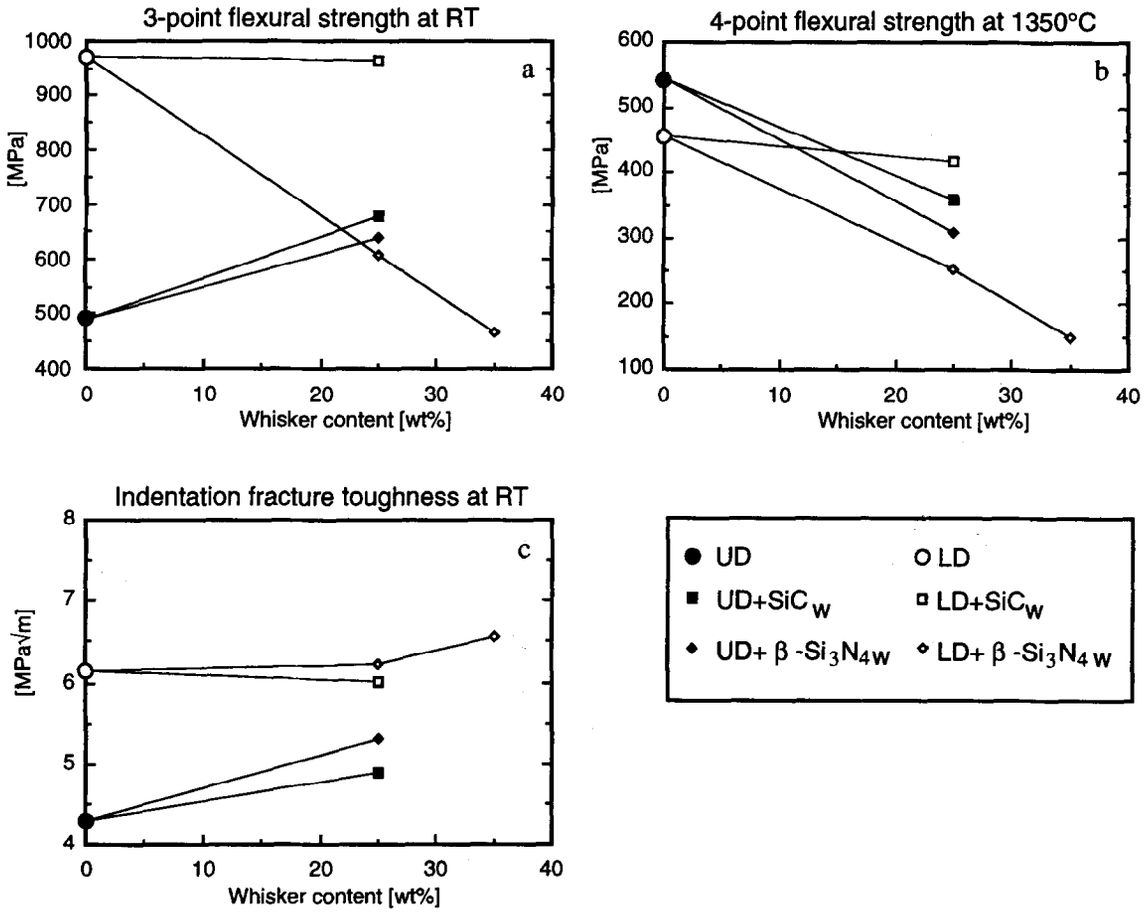

Fig. 10. (a) Three-point flexural strength at room temperature, (b) four-point flexural strength at 1350°C and (c) fracture toughness at room temperature for the examined materials.[10] The fracture toughness was determined by the indentation technique using the equation proposed by Niihara *et al.*[31]

The amount and chemistry of the residual intergranular glass may affect the contribution from different toughening and strengthening mechanisms in these Si_3N_4 ceramics. The intergranular glass also plays a vital role for the high-temperature properties. In fracture testing at 1350°C, a significant strength reduction was observed for the materials formed with metal oxide sintering additives. This can be explained by softening of the intergranular glass. The reference material formed without the metal oxide sintering additives retained its strength at elevated temperatures, Fig. 10, and this material also had the longest lifetime in stepped temperature stress rupture (STSR) tests of these materials.[10] This can be explained by the smaller volume of an intergranular amorphous phase with a different composition.

5 Concluding Remarks

Analytical electron microscopy in combination with quantitative microscopy showed that additions of SiC and β-Si_3N_4 whiskers as well as processing conditions affect the matrix microstructure of Si_3N_4-based ceramics. The different additives also influence the intergranular microchemistry, resulting in different secondary crystalline phases. Additions of SiC whiskers suppress growth of larger β-Si_3N_4 grains which results in a narrower grain size distribution. Densification of SiC reinforced Si_3N_4 ceramics without the addition of metal oxide sintering aids also results in a significantly reduced mean grain size of the β-Si_3N_4 matrix compared with that of the unreinforced material. Additions of β-Si_3N_4 whiskers promote exaggerated grain growth during densification which results in a coarser microstructure. β-Si_3N_4 whisker reinforced materials formed with metal oxides (in this case smaller amounts of Y_2O_3 and Fe_2O_3) have an apparent bimodal microstructure consisting of larger grains dispersed in a fine-grained matrix. The large β-Si_3N_4 grains in these microstructures act as flaws and lead to reduced strength. The microstructure of the unreinforced Si_3N_4 material formed with smaller additions of Y_2O_3 and Fe_2O_3 contained a fraction of larger, possibly also elongated, β-Si_3N_4 grains, despite a smaller mean grain size.

A more fibrous microstructure results in higher strength and toughness at room temperature. Addition of SiC or β-Si_3N_4 whiskers to such a microstructure may not have any significant effect on fracture toughness. The results from this investigation indicate that matrix microstructure has a significant influence on the mechanical properties of reinforced Si_3N_4 ceramics.

Acknowledgements

This work was supported by the Swedish National Board for Technical Development (STU) and the Swedish Research Council for Engineering Science (TFR). The materials and data from mechanical testing were provided by AC Cerama AB. Help with the quantitative microscopy by Dr Jonas Wasén is gratefully acknowledged.

References

1. Lange, F. F., Silicon nitride polyphase systems: fabrication, microstructure and properties. *Int. Met. Rev.*, No.1 (1980) 1–20.
2. Knutson-Wedel, E. M., Falk, L. K. L., Björklund, H. & Ekström, T., Si_3N_4 ceramics formed by HIP using different oxide additions—relations between microstructure and properties. *J. Mater. Sci.*, **26** (1991) 5574–5584.
3. Knutson-Wedel, E. M., Falk, L. K. L. & Ekström, T., Characterization of Si_3N_4 ceramics formed with different oxide additives *J. Hard Mater.* **3**[3–4] (1992) 435–445.
4. Pyzik, A. J., Carroll, D. F. & Hwang, C. J., The effect of glass chemistry on the microstructure and properties of self reinforced silicon nitride. In *Silicon Nitride Ceramics —Scientific and Technological Advances*, eds I-W. Chen, P. F. Becher, M. Mitomo, G. Petzow & T.-S. Yen. Materials Research Society, Pittsburgh, PA, 1990, pp. 411–416.
5. Lewis, M. H. & Lumby, R. J., Nitrogen ceramics: liquid phase sintering. *Powder Metall.* **26**[2] (1983) 73–81.
6. Hampshire, S. & Jack, K. H., The kinetics of densification and phase transformation of nitrogen ceramics. In *Special Ceramics* 7, eds D. Taylor & P. Popper. British Ceramic Research Association, Stoke-on-Trent, 1981, pp. 37–49.
7. Falk, L. K. L., Microstructural development of Si_3N_4 ceramics formed with additions of ZrO_2. *Mater. Forum*, **17** (1993) 83–93.
8. Buljan, S. T., Baldoni, J. G. & Huckabee, M. L., Si_3N_4–SiC composites. *Am. Ceram. Soc. Bull.*, **66**[2] (1987) 343–352.
9. Campbell, G. H., Rühle, M., Dalgliesh, B. J. & Evans, A. G., Whisker toughening: a comparison between aluminium oxide and silicon nitride toughened with silicon carbide. *J. Am. Ceram. Soc.*, **73**[3] (1990) 521–530.
10. Larker, H. T. & Adlerborn, J., Undoped and low-doped silicon nitride with whisker reinforcement made by glass encapsulated HIP. In *Ceramic Materials and Components for Engines* (Las Vegas, USA, 27–30 Nov. 1988), ed. V. J. Tennery. American Ceramic Society, Inc., Westerville, OH, 1989, pp. 227–236.
11. Hockey, B. J., Wiederhorn, S. M., Liu, W., Baldoni, J. G. & Buljan, S.-T., Tensile creep of whisker reinforced silicon nitride. *J. Mater. Sci.*, **26** (1991) 3931–3939.
12. Olagnon, C. & Bullock, E., The influence of whisker morphology on processing and toughness of a silicon nitride–matrix composite. *Silicates Ind.* **3/4** (1991) 53–60.
13. Becher, P. F., Hsueh, C.-H., Angelini, P. & Tiegs, T. N., Toughening behaviour in whisker reinforced ceramic matrix composites. *J. Am. Ceram. Soc.*, **71**[12] (1988) 1050–1061.
14. Becher, P. F., Fuller Jr, E. R. & Angelini, P., Matrix grain-bridging contributions to the toughness of whisker reinforced ceramics. *J. Am. Ceram. Soc.*, **74**[9] (1991) 2131–2135.
15. Björklund, H., Wasén, J. & Falk, L. K. L., Quantitative microscopy of β-Si_3N_4 ceramics. Accepted for publn in *J. Am. Ceram. Soc.*

16. Falk, L. K. L., Björklund, H., Adlerborn, J. E. & Larker, H. T., Grain morphology and intergranular structure of Si_3N_4 based ceramics formed by HIP. In *Ceramic Materials and Components for Engines*, eds R. Carlsson, T. Johansson & L. Kahlman. Elsevier Science Publishers, London, 1992, pp. 699–706.
17. Björklund, H., Falk, L. K. L., Adlerborn, J. E. & Larker, H. T., Grain morphology and intergranular structure of Si_3N_4 based ceramics formed by HIP. In *Silicon Nitride Ceramics — Scientific and Technological Advances*, eds I.-W. Chen, P. F. Becher, M. Mitomo, G. Petzow & T.-S. Yen. Materials Research Society, Pittsburgh, PA 1990, pp. 423–428.
18. Björklund, H., Falk, L. K. L. & Wasén, J., Characterization of the matrix morphology in Si_3N_4 ceramics formed with different additives. In *Proc. Int. Conf. on Silicon Nitride-Based Ceramics, Stuttgart*, eds M. J. Hoffman, P. F. Becher & G. Petzow. Key Engineering Materials Vols 89–91, Trans Tech Publications, Switzerland, 1994, pp. 477–482.
19. Wasén, J. & Warren, R., *A Catalogue of Stereological Characteristics of Selected Solid Bodies — Volume 1 Polyhedrons.* Department of Engineering Metals Publication, Chalmers University of Technology, Göteborg, 1990, pp. 2–8.
20. Clarke, D. R., Observations of microcracks and thin intergranular films in ceramics by transmission electron microscopy. *J. Am. Ceram. Soc.*, **63**[1] (1980) 106.
21. Wötting, G., Kanka, G. & Ziegler, G., Microstructural development, microstructural characterization and relation to mechanical properties of dense silicon nitride. In *Non-Oxide Technical and Engineering Ceramics*, ed. S. Hampshire. Elsevier Applied Science, London, 1986, pp. 83–96.
22. Abe, O., Sintering process of Y_2O_3- and Al_2O_3-doped Si_3N_4. *J. Mater. Sci.*, **25** (1990) 4018–4026.
23. Lancin, M., Ramoul-Badache, K., Kihn, Y. & Sevely, J., Phase characterization in Si_3N_4–SiC particulate composites performed by EELS in a 1MV microscope. *Phil. Mag. A*, **58**[4] (1988) 667–676.
24. German, R. M., *Liquid Phase Sintering.* Plenum Press, New York, 1985, pp. 127–155.
25. Muscat, D., Pugh, D. P. & Drew, R. A. L., Microstructure of an extruded β-silicon nitride whisker-reinforced silicon nitride composite. *J. Am. Ceram. Soc.*, **75**[10] (1992) 2713–2718.
26. Hirao, K., Nagaoka, T., Brito, M. E. & Kanzaki, S., Microstructure control of silicon nitride by seeding with rodlike β-silicon nitride particles. *J. Am. Ceram. Soc.*, **77**[7] (1994) 1852–1867.
27. Misra, A. K., Thermochemical analysis of chemical processes relevant to the stability and processing of SiC-reinforced Si_3N_4 composites. *J. Mater. Sci.*, **26** (1991) 6591–6598.
28. Karasek, K. R., Bradley, S. A., Donner, J. T., Martin, M. R., Haynes K. L. & Yeh, H. C., Composition and microstructure of silicon carbide whiskers. *J. Mater. Sci.*, **24** (1989) 1617–1622.
29. Ryabchikov, I. V., Khrushchev, M. S., Maksimov, Yu. S. & Shchedrovitskii, Ya. S., Thermodynamics of reactions of silicon carbide with the oxides of silicon and calcium. *J. Appl. Chem. USSR*, **37** (1964) 2027–2029.
30. Homeny, J., Neergard, L. J., Karasek, K. R., Donnerand, J. T. & Bradley, S. A., Characterization of β-silicon nitride whiskers. *J. Am. Ceram. Soc.*, **73**[1] (1990) 102–105.
31. Niihara, K., Morena, R. & Hasselman, D.P.H., Indentation fracture toughness of brittle materials for Palmqvist cracks. In *Fracture Mechanics of Ceramics* 5, ed R. C. Bradt, D. P. H. Hasselman & F. F. Lange. Plenum Press, New York, 1983, pp. 97–105.
32. Björklund, H. & Falk, L. K. L., Matrix morphology and mechanical properties of whisker reinforced Si_3N_4 ceramics. *Silicates Ind.*, **1/2** (1996) 45–52.
33. Becher, P. F., Lin, H. T., Hwang, S. L., Hoffmann, M. J. & Chen, I.-W., The influence of the microstructure on the mechanical behaviour of silicon nitride ceramics. In *Silicon Nitride Ceramics — Scientific and Technological Advances*, eds I.-W. Chen, P. F. Becher, M. Mitomo, G. Petzow & T.-S. Yen. Materials Research Society, Pittsburgh, PA, 1990, pp. 147–158.